Hydration characteristics and durability of Ground Granulated Blast Furnace Slag - Homra geopolymer cement

Amira A.Elsaman, E. E. Hekal, F. S. Hashem, F. A. Selim

Abstract

In this paper; Ground Granulated Blast Furnace Slag (GGBFS) used to produce geopolymer cement (GPC) at ambient temperature and 100% relative humidity, the influence of replacing slag by 10, 20 and 30% of brick wastes (Homra) as well as the effect of sodium silicate to sodium hydroxide ratio (SS:SH), 2, 1 and 0.5 by weight in the alkaline activator solution on the properties of the produced geopolymer have been investigated. This was done through measurement of compressive strength values, setting times, water absorption as well as performing FTIR spectra, XRD patterns and microstructure development is investigated using SEM imaging. It is concluded that from the results, the optimum percentage replacement of GGBFS with Homra is 10%. Besides, the optimum SS:SH ratio is 1 by weight. Initial and final setting times increase with decreasing the SS:SH ratio for all tested pastes. Replacing GGBFS with different amount of Homra causes a notable increase in both initial and final setting times for GPC specimens made by SS/SH ratio of 2. Water absorption of the formed geopolymers decreased with increasing SS:SH ratio from 0.5 to 1 then showed a slight increase with a further increase to 2. Also this paper presents an experimental study resistance of GPC to sulfate attacks where partial replacement of GGBFS by 10% homra give high strength value than 100% GGBFS as a result of immersion in sulfate solution.

Keywords: Alkaline activation, Alkaline activators, Cement industry, Geopolymer cement, Geopolymerization, Ground Granulated Blast Furnace Slag, Homra,

1. Introduction

Cement is considered as the most commonly used binder in the construction industry. The production of Portland cement is consumed high amount of energy and produce high green house gas [1], where production one ton of Portland cement generate almost one ton of CO_2 [2]. The contribution of Portland cement production to emission greenhouse gas is about 6% of the total greenhouse gas produced in the world [3].

Geopolymers are great interest as binders with low emission of CO_2 if comparison with OPC. Geopolymers are a very promising kind of material since they have been shown to offer an environmentally friendly [4–6], where manufacture of geopolymer produces five times CO_2 less than does the manufacture of Portland cement, so it has been proposed to be an alternative to Portland cement concrete (PCC). Actually, geopolymers are kinds of inorganic polymers, it is a class of three-dimensionally networked alumino-silicate materials, similar to zeolite and first developed by Joseph Davidovits in 1978 [7,8]. Fly ash based geopolymer was the first introduced by Davidovits in 1979 to reduce the use of OPC in concrete [9]. Many authors made comparison between zeolite chemistry and geopolymer chemistry due to the similarities between them [10-13]. The mechanism involves the dissolution of Al and Si in the alkali medium, transportation (orientation) of dissolved species and polycondensation, forming 3D network of silico-aluminate structures [14]. The research in geopolymer includes thermal behaviour [15], durability in sodium and magnesium sulfate solutions [16], and resistance to acid attack [17] of geopolymeric materials. The use of GGBFS as cement replacement material in geopolymer concrete reduces the emission of CO_2. [18,19] showed that alkali-activated slag concrete had lower resistance to alkali-aggregate and carbonation than that of OPC concrete.

[20, 21] made combination of raw waste materials like fly ash and slag with low concentration alkaline activators (e.g. potassium hydroxide + potassium silicate); as well as curing at room temperature. The parameters affected on the hardening rate of fly ash geopolymer and change the setting time from minutes to days are the type, dosage, concentration of alkali metal activator (Na or K), temperature of curing [22-26]. The percentage of different reaction products depends on various factors as alkalinity, temperature, calcium sources, rate of dissolution of ions from aluminosilicate and ratio of aluminosilicate to calcium sources [27–30]. [31-35] indicated the effects of calcium ion on early age (loss of workability) as well as later age properties (high strength) of metakaolin or fly ash based geopolymer. [27,36] reported the metakaolin and slag blends towards the coexistence of geopolymeric gel and calcium silicate hydrate. Several papers measured the setting times of fly ash, metakaolin or slag-based geopolymers using a Vicat penetrating needle (ASTM C191) [23, 25, 35, 37–40]. Shi et al [41] showed that alkali-activated slag concrete had higher strength development and better durability than that of Portland cement concrete. In some cases, it has been shown that one day strength and three days strength is 68 MPa and 96 MPa respectively [42-44].

In this paper ground granulated blast furnace slag and clay - bricks (Homra) wastes were used as industrial raw materials to produce geopolymeric green cement using (sodium silicate (SS) and sodium hydroxide (SH)) as alkaline activator with different LSS:LSH mass ratio at ambient temperature and 100% relative humidity conditions and also measuring of durability gainst magnesium sulfate solution and thermal resistance of geopolymer cement pastes.

H1.3	90	10	1	2	0.5
H2.1	80	20	2	1	2
H2.2	80	20	1	1	1
H2.3	80	20	1	2	0.5
H3.1	70	30	2	1	2
H3.2	70	30	1	1	1
H3.3	70	30	1	2	0.5

2. Experimental

2.1. Materials

The raw materials used in this investigation are Ground Granulated Blast Furnace Slag (GGBFS), which is a by-product of iron production provided from Iron and Steel Company, Helwan governorate of Blain surface area 2275 cm^2/g and Crushed clay bricks (Homra) of Blaine surface area 5053 cm^2/g. The chemical oxide composition for (GGBFS) and Homra are given in Table 1.

Table 1: Chemical oxide compositions of raw materials.

Materials	Oxides (mass,%)								
	SiO_2	Al_2O_3	Fe_2O_3	CaO	MgO	SO_3	K_2O	Na_2O	LOI
GGBFS	37.6	10.9	0.6	35.7	8.26	1.71	0.97	1.28	2.98
Homra	67.37	13.28	6.86	2.72	1.67	1.08	0.9	1.21	4.91

Alkaline Activated Solution (AAS) used in this investigation is a mixture of Sodium Silicate ($Na_2SiO_3.9H_2O$, 6M) and Sodium Hydroxide (NaOH, 10M). Distilled water is used to prepare the alkaline activator solution. The required weight ratio of sodium silicate and sodium hydroxide solutions are mixed before adding to the dry raw materials.

Magnesium sulfate ($MgSO_4$) is used as source of sulfate in durability test. All chemicals were Alfa aromatic Company.

2.2 Sample preparation

The dry mixes with the required composition (as mentioned in Table 2) were prepared by mixing the solid raw materials in ball mill for 6 hours to occurred complete homogeneity.

Table 2: The percentage compositions of the different geopolymer mixes and their designations.

Mixes	GGBFS	Homra	LSS,%	LSH,%	(LSS / LSH, %) (Na_2SiO_3 / NaOH
B1.1	100	-	2	1	2
B1.2	100	-	1	1	1
B1.3	100	-	1	2	0.5
H1.1	90	10	2	1	2
H1.2	90	10	1	1	1

Geopolymer cement pastes (GCP) were prepared by mixing the dry sample with the calculated amount of alkaline activator (6M Na_2SiO_3 and 10M NaOH). The mass ratio of solid raw materials to alkaline activator solution used (S: A) is 2:1, while the ratios of Na_2SiO_3 (LSS) to NaOH (LSH) to form alkaline activator are (2, 1 and 0.5%).

The resulted pastes were molded into cubic specimens by using cubic moulds have one-inch dimension. The moulds were compacted via vibration; the leveling and smoothness of the top surface of the pastes were done by thin edged towels. Then the pastes were removed from their moulds and cured at ambient temperature at about 100% relative humidity for 3, 7, 14, 28 and 90 days.

After 28 days of curing in 100% RH made durability test by taking certain numbers of cubes and immersed in 5% $MgSO_4$ solution. Then, these cubes were tested by compressive strength machine after 1, 2, 4 and 6 months of curing in 5% $MgSO_4$ solution. Also made thermal resistance After 28 days of curing in 100% RH, certain number of cubes were dried at 80 °C for 24 hrs, and then fired at 200 °C, 300 °C and 600 °C, the weight before and after firing was taken.

2.3. Testing and characterization

The cubic specimens were used for the determination of the compressive strength after each curing age; the average of the three reading of compressive strength was considered. These specimens represented a certain composition and cured for a certain period. The compressive strength test was performed using a ton industry machine (West Germany). Stopping the geopolymerization process at each curing time was done by removing the free water; this was accomplished by drying the crushed specimens for 24 hours at 105 °C [45]. The initial and final setting times for each freshly prepared paste were determined using Vicat needle [46]. Water absorption measurements of the hardened geopolymer specimens were carried out according to ASTM C140 [47].

The percentage of absorption was calculated using the following equation:

Water Absorption (%) = [(W1-W2) / W2] x 100   (1)

Where:

W1: The weigth of the surface dry sample after immersion in water for at least 24 hours.

W2: The weight of specimen after complete drying at 105 °C .

X-ray diffraction technique was carried out of some selected hydrated and dried geopolymer pastes to investigate the crystallinity structure and mineralogy of these mixes.

The spectroscopic analysis was performed of some selected hardened geopolymer pastes to evaluate the functional groups in the hardened geopolymer samples using Fourier Transformation Infrared (FTIR). The band spectral was recorded in the range of 4000 – 400 cm^{-1}. Scanning electron microscope; (SEM) has been used to study the morphology and microstructure of some selected GPC specimens.

3. Results and discussion

3.1. Compressive strength

The compressive strength values for 100% GGBFS based geopolymer cement (GPC) hardened specimens and pastes replaced by 10, 20 and 30% of homra, prepared using solid / activator (S:A) ratio of 2:1 and sodium silicate/sodium hydroxide (LSS:LSH) ratio of 2 (mixes (B1:1, H1:1, H2:1 and H3:1 respectively) after 3, 7, 14, 28 and 90 days of curing at ambient room temperature and 100% relative humidity are shown in Fig. 1.a. The compressive strength values indicated a continuous increase with increasing the age of curing for all specimens (mixes B1:1, H1:1, H2:1 and H3:1). In addition; as the replacement of homra increase as the compressive strength values decrease. And the replacement of 10% homra show the highest compressive strength value especially at later ages of curing. The increasing of the compressive strength values due to the formation of geopolymer with good mechanical properties via the alkali activation of GGBFS. This results can be explained in terms of the higher reactivity of GGBFS, which in the presence of the alkaline activator (OH$^-$) which promote the rupture of bonds in its structure (Ca-O, Si-O and Al-O) that forms dissolved species (Ca^{2+}, (H$_2$SiO$_4$)$^{2-}$, (H$_3$SiO$_4$)$^-$ and (Al(OH)$_4$)$^-$ which can precipitate when reaches to saturation to form CSH and CASH [48]. Also the calcium ions present in slag enter in the Si-O-Al structure, which compensate the charge of the aluminum atoms (Al)$^{3+}$ and allows the space for the CASH in addition to NASH gel this leads to formation of more dense structure [49,50]. The decrease in the compressive strength values for mixes replaced by 20 or 30% of homra due to the increase in the amount of unreacted silicon by the presence of high amount of homra; which has a deleterious effect on the mechanical strength of geopolymers [51].

Fig.1 (b and c) show the compressive strength values for 100% GGBFS based geopolymer cement (GPC) hardened specimens and pastes replaced by 10, 20 and 30% homra GPC specimens by using solid / activator (S:A) ratio of 2:1 and sodium silicate/sodium hydroxide (LSS:LSH) ratios of 1 and 0.5 mixes [(B1:2, H1:2, H2:2 and H3:2) and (B1:3, H1:3, H2:3 and H3:3)], respectively after 3, 7, 14, 28 and 90 days of curing at ambient room temperature and 100% relative humidity. The compressive strength values show almost the same trend as in the Fig. 1.a; where there is a continuous increase with increasing the age of curing for all GPC specimens. Also, as the replacement of homra increases as the compressive strength values decrease. And, the replacement of 10% homra shows almost the highest compressive strength value especially at later ages of curing; the reasons for these results were discussed in the previous section.

By comparison all the figures of compressive strength Fig.1.a, Fig.1.b and Fig.1.c to show the effect of different ratios of activators (SS/SH = 2, 1 and 0.5). Obviously, as the ratio of SS/SH decrease from 2 to 1 as the values of compressive strength increase and decrease again as the ratio of sodium silicate/sodium hydroxide decrease from 1 to 0.5. So, the lowest compressive strength values for GPC specimens at all ages of curing made by using ratio of activator (SS/SH= 0.5); where it is the highest content of sodium hydroxide used among the other SS/SH ratios, indicated the lowest geopolymerization reaction. Evidently; if the alkalinity is low (high SS/SH ratio) the dissolution of calcium ions Ca^{2+} from slag is promoted and consequently the formation of CSH gel is pronounced, leading to stable gel coexistence, but high alkalinity (low SS/SH ratio) tends to lead for Ca(OH)$_2$, where it has low hydraulic property [52].

Obviously; for GPC specimens prepared by using alkaline activator (SS/SH) mass ratio of 1 the geopolymer indicated a relatively high strength values during all curing periods for all GPC specimens due to the complexity of the geopolymerization process and indicated the effect of the concentration of the alkaline activator constituents and the presence of dissolved silicon in the aqueous solution of sodium silicate contributes to the increase of compressive strength. The higher concentration of dissolved silicon produces higher compressive strength values, but only for certain limit, further increase in silicon ions concentration causes a notable decrease in the compressive strength values [53]. Many papers have suggested that the optimum SS:SH ratio to produce geopolymer having high strength values is in the range 0.67–1.00 [50] , as mentioned in this study. In general, the use of sodium silicate helps to improve and increase the rate of the geopolymerisation process by accelerating the dissolution of the source material. These results are in agreement with the previous results in the papers [5,54]. And; the slight decrease in the compressive strength values observed with increasing SS:SH ratio to 2 in the alkaline solution, is mainly attributed to increasing the viscosity of the reaction matrix with increase SS:SH ratio and thus hindered the mass transport through the solution which leads to a low strength of

geopolymer paste. Moreover, increasing the amount of unreacted material, which increases with silicon concentration and has a deleterious effect on the mechanical strength of geopolymers [51,55]. On conclusion, in this study, the obtained results revealed that the compressive strength of the formed geopolymers increases for SS:SH ratio of 1, due to the promotion of polymerization reaction.
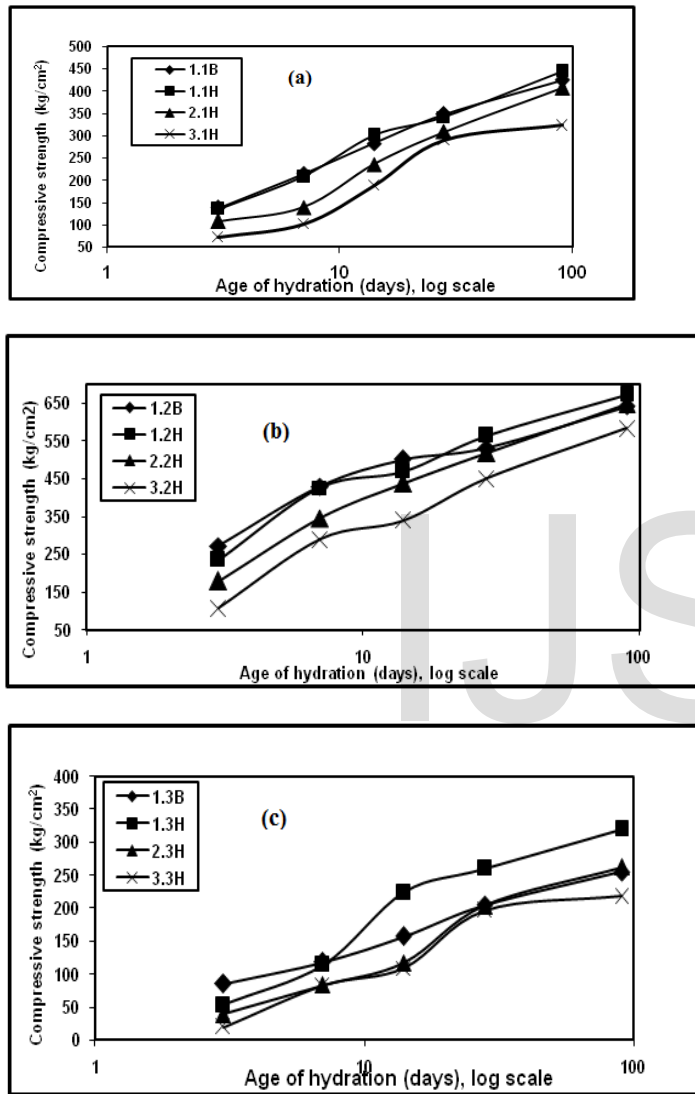

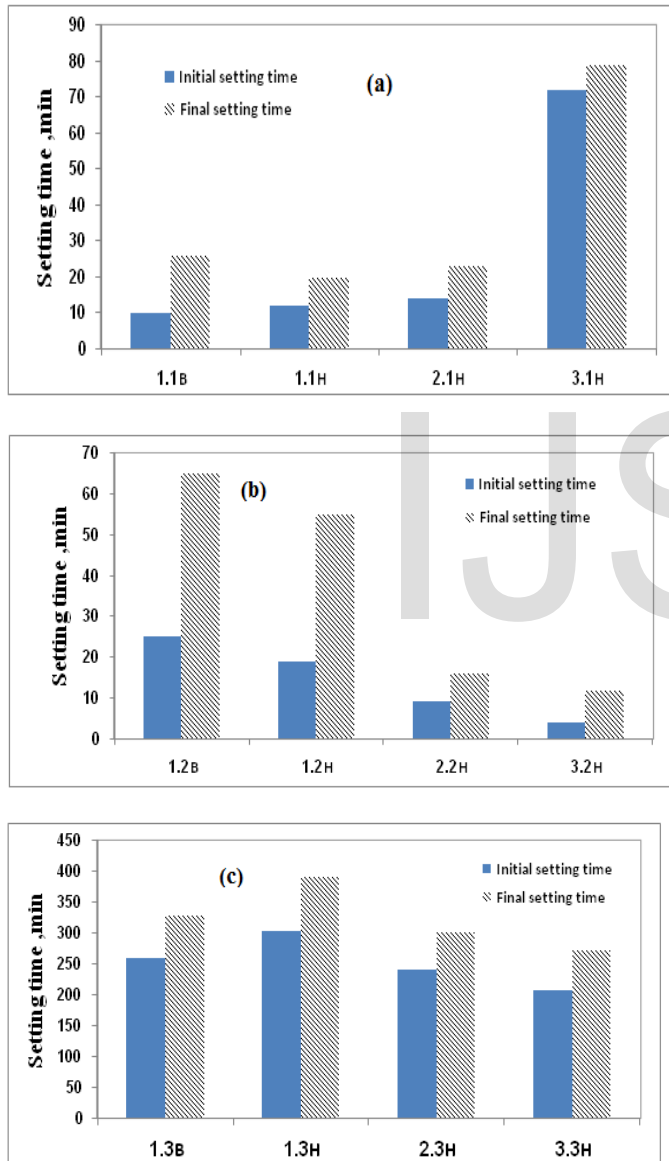**Figure**. 1. Compressive strength values of GPC specimens made from Mixes (B1.1, H1.1, H2.1 and H3.1), Mixes (B1.2, H1.2, H2.2 and H3.2) and Mixes (B1.3, H1.3, H2.3 and H3.3) after different ages of curing.

3.2. Setting Times

The results of the initial and final setting times for 100% GGBFS based geopolymer cement (GPC) hardened specimens and pastes replaced by 10, 20 and 30% homra, prepared using solid / activator (S:A) ratio of 2:1 and sodium silicate/sodium hydroxide (SS:SH) ratio of 2, 1 and 0.5 mixes [(B1:1, H1:1, H2:1 and H3:1),

(B1:2, H1:2, H2:2 and H3:2) and (B1:3, H1:3, H2:3 and H3:3)], respectively are shown in Fig. 2. (a, b and c). The initial setting times ranges from 4 to 304 min while the final setting time ranged from 12 to 391 min. Clearly, the results revealed that the initial and final setting times are affected by two main factors namely (1) Sodium silicate: Sodium hydroxide ratio and (2) The % replacement of GGBFS by Homra. Obviously, the results showed a notable increase in both initial and final setting times values with decreasing the SS:SH ratio for all tested pastes. Obviously, GPC specimens made with least amount of sodium silicate (SS/SH ratio of 0.5) have the largest initial and final setting times compared to those made with larger SS/SH ratios, (1 and 2). This result is due to the reduction in the amount of Si present in the paste, which results in slowing the polymerization process [56]. Decreasing the ratio SS:SH in the alkaline activator solution increased setting times which due to increasing the rate of geopolymerisation [57]. These results illustrate the influence of chemical compositions of alkaline activator on the rate of setting. Evidently, upon decreasing the SS:SH ratio from 2 to 0.5, the amount of soluble silica decrease, the polymerization process is retarded so, the initial and final setting times increased. Replacing GGBFS with different amount of Homra (10, 20 and 30% by mass of slag) causes a notable increase in both initial and final setting times for GPC specimens made by SS/SH ratio of 2, where there is large increase in setting times for pastes made by replacing of 30% homra due to retardation of the rate of polymerization process in the presence of these waste materials. But there is a notable decrease in both initial and final setting times for GPC specimens made by SS/SH ratio of 1 and 0.

3.3. Water absorption studies

The results of water absorption values for 100% GGBFS based geopolymer cement (GPC) hardened specimens and pastes replaced by 10, 20 and 30% homra, prepared using solid / activator (S:A) ratio of 2:1 and sodium silicate/sodium hydroxide (SS:SH) ratio of 2, 1 and 0.5 after 3, 7 14 and 28 days of curing at ambient temperature mixes [(B1:1, H1:1, H2:1 and H3:1), (B1:2, H1:2, H2:2 and H3:2) and (B1:3, H1:3, H2:3 and H3:3)], respectively are given in Fig. 3. (a, b and c). This test was used to investigate the relative porosity or permeability of the hardened GPC pastes.

It was clear that the water absorption values for all GPC specimens decrease with increasing the curing times due to formation of more hydration products in the pores. The GPC paste made from 100% GGBFS show the lowest water absorption values especially when used low SS/SH ratio, (1 and 0.5) this is due to continuous activation of slag hydration by activators and accumulation of hydration products which fills some of open pores and due to reduction of porosity in presence of slag due to formation of new phases in geopolymer pasted. Beside, the mix made from replacement of slag by 10% homra showed the lowest water absorption values than those of replaced by 20 or

30% homra, suggesting that the 10% homra wt., % was the optimum percentage for the replacement of GGBFS. These results are in agreement with the results of compressive strength obtained, which indicated higher compressive strength values for these mixes, due to a low degree of porosity [52]. It was clear from the results of water absorption that the values of water absorption for GPC specimens made by using SS/SH ratio of 1 almost the lowest water absorption values than the other ratios of SS/SH these results are in agree with the obtained compressive strength results.

Figure. 2. Mass change of GPC specimens made from Mixes (B1.1, H1.1, H2.1 and H3.1), Mixes (B1.2, H1.2, H2.2 and H3.2) and Mixes (B1.3, H1.3, H2.3 and H3.3) after different ages of curing.
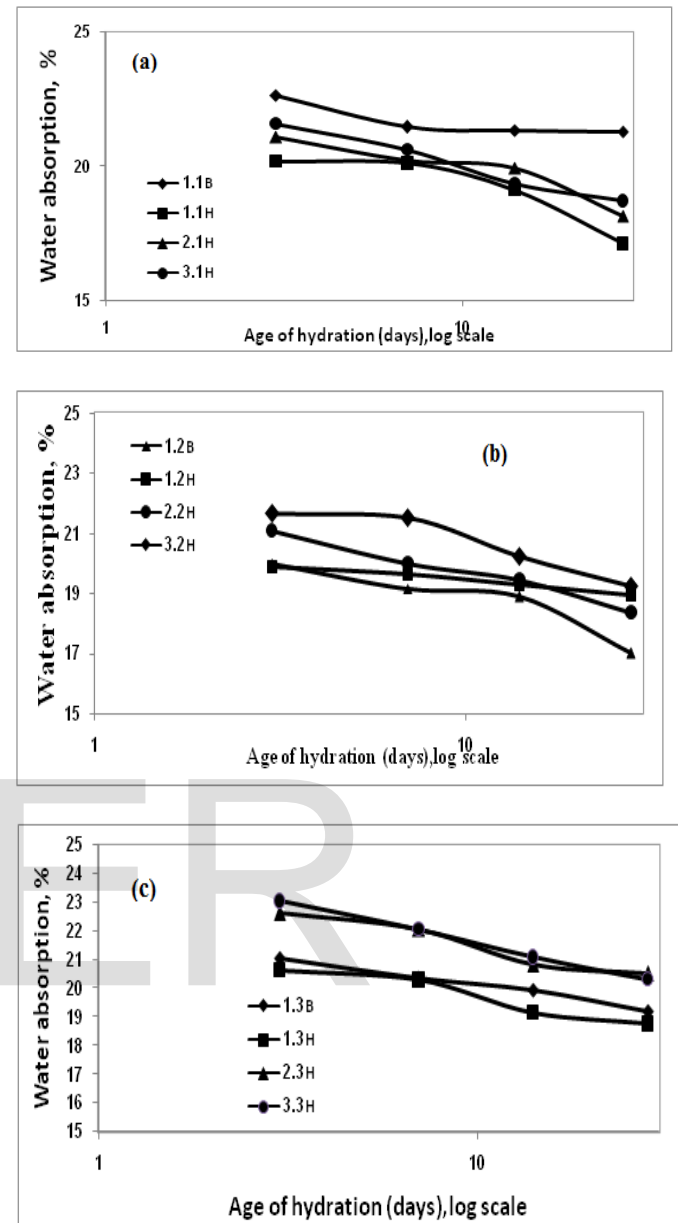
Figure. 3. Water absorption of GPC specimens made from Mixes (B1.1, H1.1, H2.1 and H3.1), Mixes (B1.2, H1.2, H2.2 and H3.2) and Mixes (B1.3, H1.3, H2.3 and H3.3) after different ages of curing.

3.4. Resistance to Sulfate attack

Sulfate attack resistance is an important durability test for materials used in construction. Two geopolymer cement specimens, (B1.2 and H1.2) were used to evaluate magnesium sulfate resistance. The Compressive strength of B1.2 and H1.2 mixes after immersing in 5% $MgSO_4$ for1, 2, 4 and 6 months are graphically represented in Fig. 4.

The evaluated property in this study is compressive strength. Decrease in the value of strength may be attributed to the presence of micro cracks as a result of gypsum and ettringite

formation in the pores in addition to migration of alkalis from geopolymers into the solution within pores [58] and [59]. Also found that partial replacement of GGBFS by 10% homra give high strength value than 100% GGBFS as a result of immersion in sulfate solution. This can be attributed to the partial filling of the pores by Homra which decrease the permeability and entrance of SO_4^- ions inside the core structure of geopolymers.
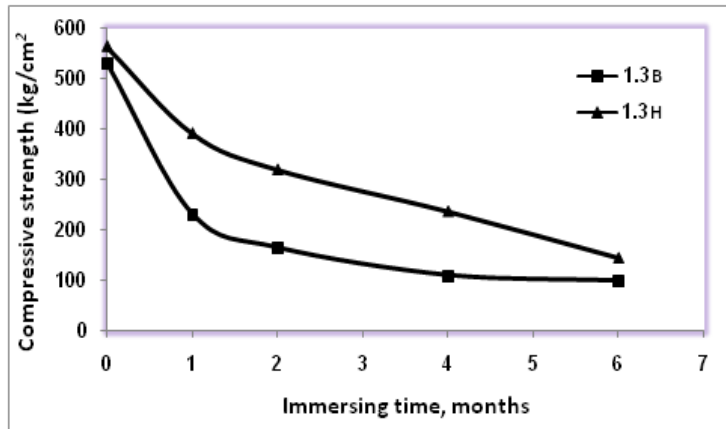

Figure (4): Compressive strength versus immersing time in 5%$MgSO_4$ for mixes B1.3 and H1.3.

3.5. Thermal effect:

The Compressive strength of B1.2 and H1.2 mixes after firing at 200 °C, 300 °C and 600 °C for 3hrs are graphically represented in Fig. 5. (a). Also, % of weight loss of B1.2 and H1.2 mixes after firing are graphically represented in Fig. 5. (b)

Firing geopolymer specimens (mixes B1.2 and H1.2) showed a sharp loss in compressive and weight. This loss continued by the increase in the firing temperature from 200 °C to 600°C for the two geopolymer specimens. The compressive strength decreased due to the increasing cracks and pores arising from the dehydration [60] According to the literature, strength deterioration appears to be a universal thermal behaviour for sodium silicate activated geopolymer compositions, such as mortars and concrete, and has been observed in slag-based geopolymer [61], [62] and [63].Weight loss is observed due to the rapid evaporation of free water that is adsorbed on the surface of grains, which may cause a nominal shrinkage.

3.6. XRD analysis

The XRD patterns of GPC specimens made from Mixes B1.2 and H1.2 after 3 and 28 days of curing in 100% RH, are shown in Fig. 6. The diffraction patterns of all mixes have a large diffused hump in the region of 27– 33° the hump at about 29° is characterizing for glassy phase of the hydration product formed

mainly as CSH gel [64,65]. The intensity and the degree of broadening of this hump are increased by increasing the amorphous CSH content of the geopolymer formed [66]. Where replacement of GGBFS by 10% homra showed increase in the intensity of this peak especially at later ages of curing (28 days), these explained the higher in the compressive strength value of mix H1.2 than blank. There is appearance of new peaks in the XRD patterns in the mix containing homra which characteristic for calcite and quartz, the appearance of calcite is due to the carbonation of the geopolymer specimens. There are appearance of another peak at about 31° corresponding to calcium aluminum magnesium silicate and peak at about 33° corresponding to aluminosilicate, and there is another peak at about 36° for mix H1.2 only after 28 days of curing which is corresponding to serendibite. XRD of mixes B1.2 and H1.2 after 1 and 4 months of immersing in 5% $MgSO_4$ are shown in Fig. 7. There are almost the same peaks of CSH, calcite and quartz, it is clear from Fig. 7. that the broadening of CSH peak increase for mix containing homra, where the presence of homra in GPC specimens made resistance to sulfate attack and increase the value of compressive strength, these results agree with the results of compressive strength development obtained. And XRD of mixes B1.2 and H1.2 after firing at 200°C and 600°C are shown in Fig. 8. It is shown from this figure that the broadening of hydration product peak as sodium calcium silicate of blank mix was higher than mix containing homra, so the compressive strength of blank is higher than B1.2 mix.

3.7. Fourier Transform Infrared (FTIR) spectroscopy analysis

Fig. 9, 10 and 11 showed the IR spectra of geopolymer samples prepared using 1 SS/SH ratio (B1.2 and H1.2) after 3 and 28 days of curing at ambient temperature and 100% relative humidity, GPC samples (B1.2 and H1.2) after firing at 200 and 600 °C and GPC specimens (B1.2 and H1.2) after immersing in 5% $MgSO_4$ solution for 1 and 4 months, respectively. All figures of tested GPC specimens showed broad band appearing at 3440 cm⁻¹, where the stretching vibrations of O-H and H-O-H appear at about 3440 cm⁻¹ and 2380 cm⁻¹. In addition, the weak band at about 1660 cm⁻¹ is associated to vibrations of OH and HOH bonds in the water molecules. In the previous studies showed that the bands as reported by Tho-In et al. [67] revealed that the water molecules were absorbed on the surface or embedded in the pores during the process of geopolymerization in hydrated products as C-S-H and C-A-S-H [68,69]. The band at roughly 1450 cm⁻¹ indicated the stretching vibration of O-C-O was detected for all tested GPC pastes which is attributed to the carbonation reaction. The carbonation process occurred due to reaction of alkali metal hydroxides (present as activator solution) with atmospheric CO_2 [70,71].

In addition the stretching vibration of Si-O-Si and Al-O-Si was detected at about 960 cm^{-1} indicated the formation of aluminosilicate gel. Also was found stretching vibration of Si-O-Si at 660 cm^{-1} and bending vibrations of Si-O-Si and O-Si-O located at 450 cm^{-1}. From Fig.9 the IR patterns showed a notable increase in the intensity of C-A-S-H and CSH gel, indicating increase in the amount of geopolymer formed with substitution of GGBFS by 10% homra, these results agree with the results of compressive strength obtained for these mixes. Also, the increase in the intensity of broad bands of stretching OH and bending HOH vibration of bound water molecules of these mixes observed in the FTIR specta in the region of 3440 to 1660 cm^{-1}, this confirmed that the geopolymers able to absorb water in three dimensional frame network increases with replacement of slag by homra. Fig.10 showed the behavior of firing GPC specimens at 200 and 600 °C the FTIR patterns showed a notable increase in the intensity of C-A-S-H and CSH gel, indicating increase in the amount of geopolymer formed with substitution of GGBFS by 10% homra and also with increasing the firing temperature. Fig.11. showed the durability behavior of tested mixes where intensity of beaks increase with increasing immersing time in sulphate solution and by replacement with 10% homra.
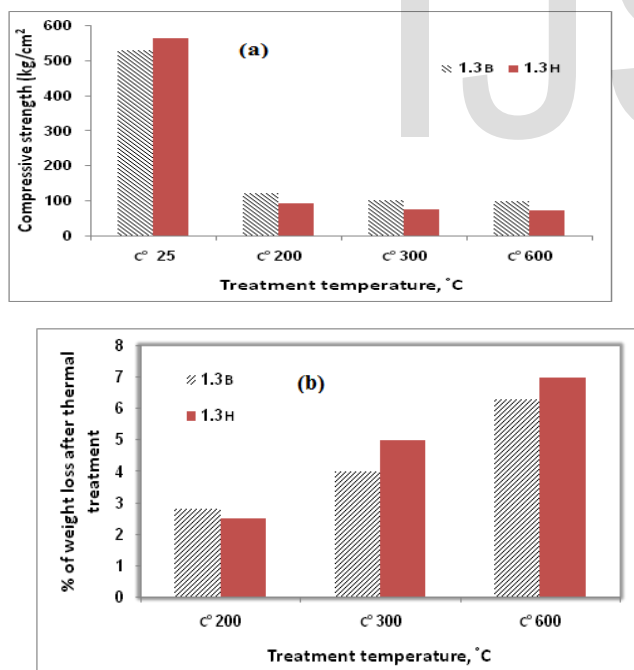

Figure.6. XRD patterns of mixes B1.2 and H1.2 after 3 and 28 days of curing in 100% RH.

Figure.7. XRD patterns of mixes B1.2 and H1.2 after 1 and 4 months of immersing in 5% MgSO$_4$ solution.

Figure.5. Compressive strength for mixes B1.3 and H1.3 versus firing temperature and the % of weight loss of mixes B1.3 and H1.3 versus firing temperature.
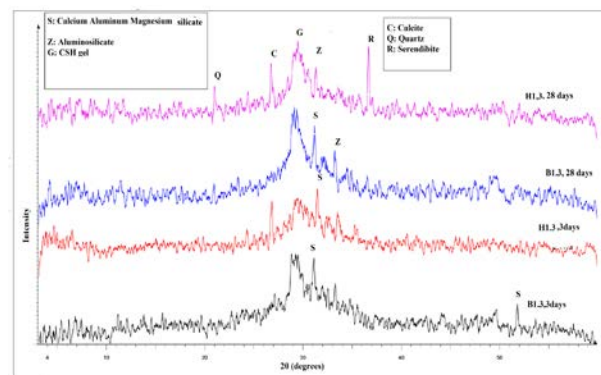

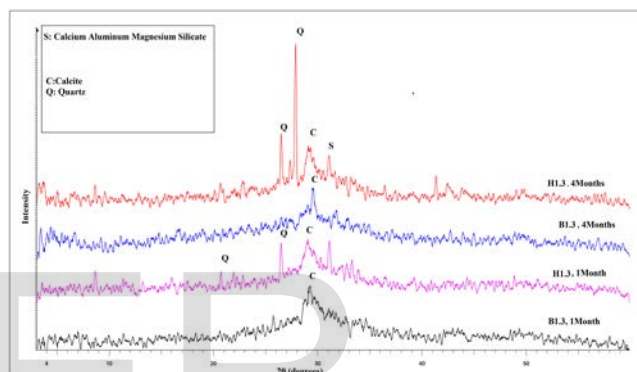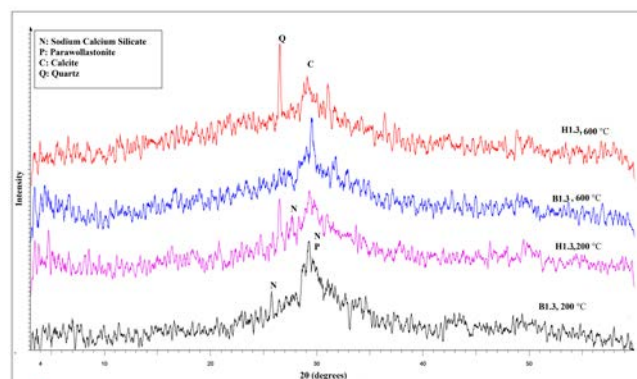**Figure.8.** XRD patterns of mixes B1.2 and H1.2 after firing at 200°C and 600°C.
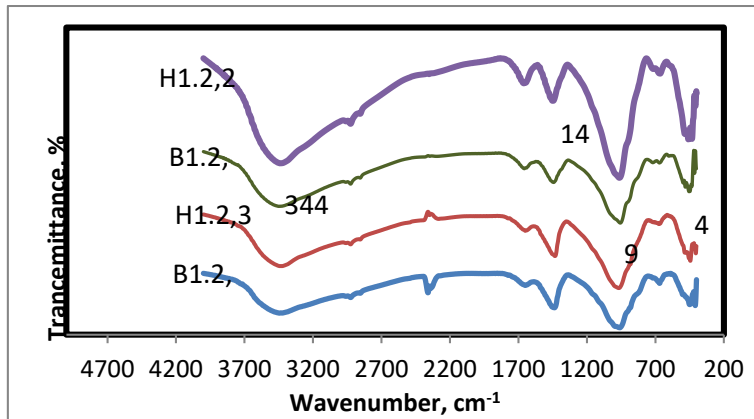
Figure.9. IR spectra of mixes B1.2 and H1.2 after 3 and 28 days of curing in 100% RH.
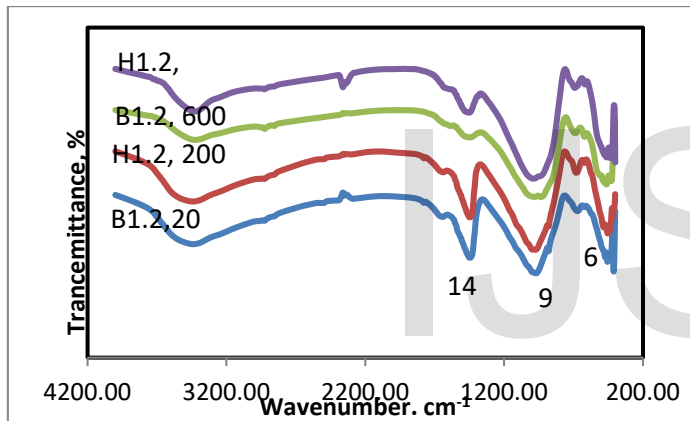

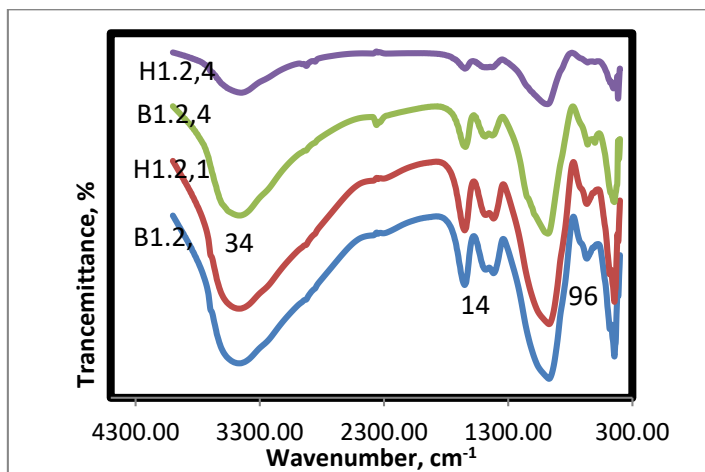**Figure.10.** IR spectra of mixes B1.2 and H1.2 after firing at 200°C and 600°C.

Figure.11. IR spectra of mixes B1.2 and H1.2 after 1 and 4 months of immersing in 5% MgSO₄ solution

3.8. Morphology and microstructure

The microstructure of the hardened geopolymer pastes prepared by using 1- SS: SH ratio (B1.2 and H1.2) after 3 and 28 days of curing at ambient temperature and 100% relative humidity, GPC specimens (B1.2 and H1.2) after immersing in 5% MgSO₄ solution for 1 and 4 months and GPC samples (B1.2 and H1.2) after firing at 200 and 600 °C are shown in Fig. 12-14, respectively. For all pastes, the SEM micrographs indicated the formation of geopolymer with mostly amorphous structure. Fig. 12. a and b. show SEM for 100% GGBFS (B1.2) after 3 and 28 days respectively, of curing in water which had continuous compact structure [72] with dense gel like matrix with structure of hydration products as calcium alumino silicate hydrate (CASH) with micro fibrous crystals of CSH [66]. Also the unreacted slag particles appear on the surface of the dense geopolymer structure. Observed that continuous geopolymerization process has been able to produce the gels where large pores tend to reduce in small and volume for long term specimen. Linking of geopolymer gels have formed capillary gels in pores and cracks [73]. Fig. 12. c and d. show SEM for GCP having 10% homra (H1.2) after 3 and 28 days respectively, of curing in water, where it is more compact and less pores than that 100% GGBFS (B1.2) [74]. The unreacted brick particles were observed with many voids in the geopolymer matrix with more compact matrix and hence, higher compressive strength. On the other hand, denser structure was observed due to the higher Na₂O content in the geopolymer mixture; this enhanced the geopolymerization and increases the compressive strength. An increase in the curing period also enhanced the arrangement of the geopolymer structure effectively. As illustrated in Fig. 12. b and d, needle-like products observed in the matrix hinted the presence of crystal phases of geopolymer matrix in the early age. As the curing period increase to 28 days, the compressive strength of the specimen increases while the needle-like products observed decreased significantly.

Obviously, these results confirmed the obtained results of compressive strength mentioned previously.

The SEM micrographs of the GPC specimens of mixes (B1.2 and H1.2) after immersion in 5% MgSO₄ solution for 1 and 4 months showed in Fig. 13, it is showed from these figures that the SEM micrographs of 100% slag mix show some needle like crystals of ettringite phase, in addition to CSH phases. The formation of ettringite which characterized by its large volume can cause an internal stress inside the pores. This internal stress leads to formation of micro-cracks, hence compressive strength decreases. SEM micrograph of mix H1.2 after curing in sulphate solution (Fig. 13. c and d) showed some small crystals of ettringite besides calcium silicate hydrates. Large rod crystals of ettringite can be identified.

The SEM micrographs of the GPC specimens of mixes (B1.2 and H1.2) firing at 200 and 600 °C are shown in Fig. 14. It is showed from these figures that there is cracking and flakiness

Figure.13. The SEM-micrographs of B1.2 and H1.2 mixes after 1

and 4 months of curing in 5% MgSO$_4$ solution
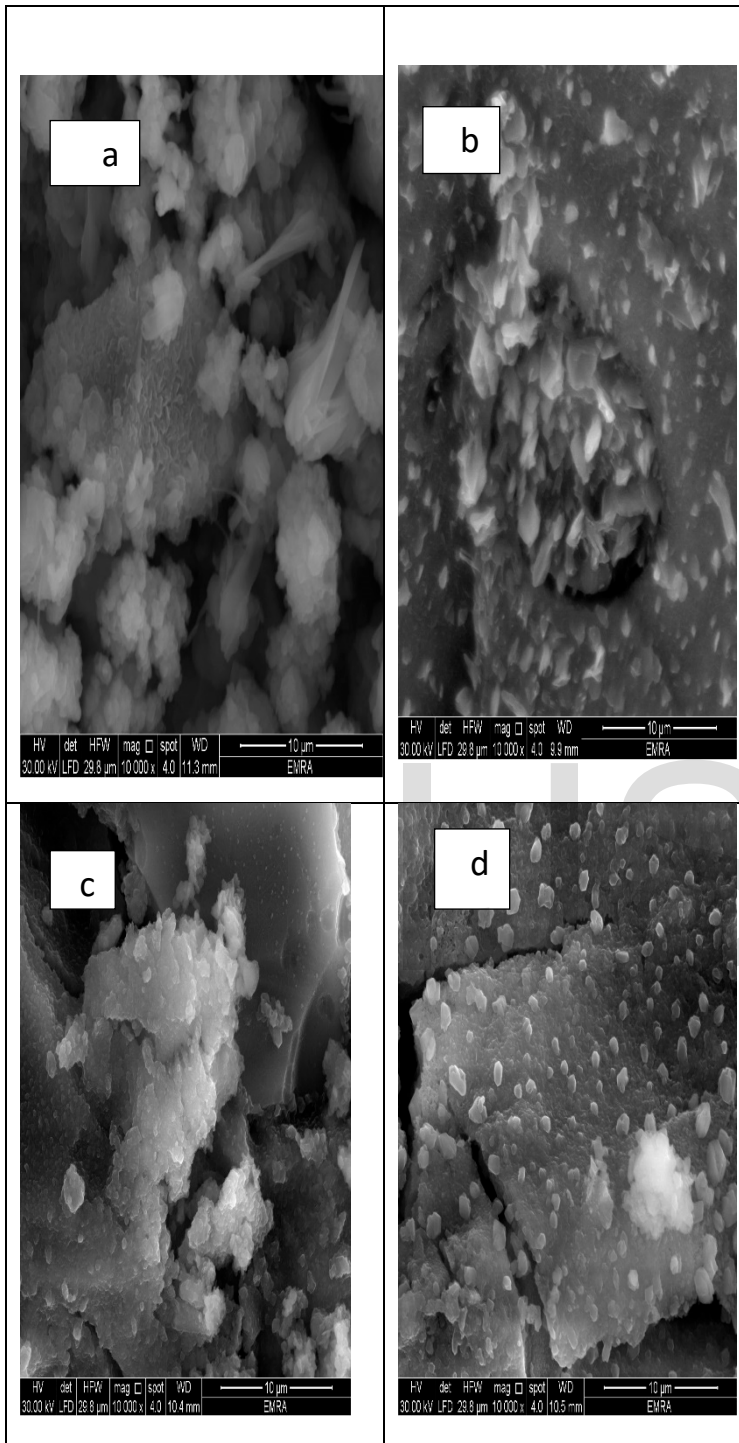
when made firing to GPC specimens which is caused decrease in compressive strength, where firing at high temperature made high degree of flakiness which decrease the compressive strength, these results agreed with the results of compressive strength mentioned previously.

Figure.12. The SEM-micrographs of B1.2 and H1.2 mixes after 3 and 28 days of curing in 100% RH.
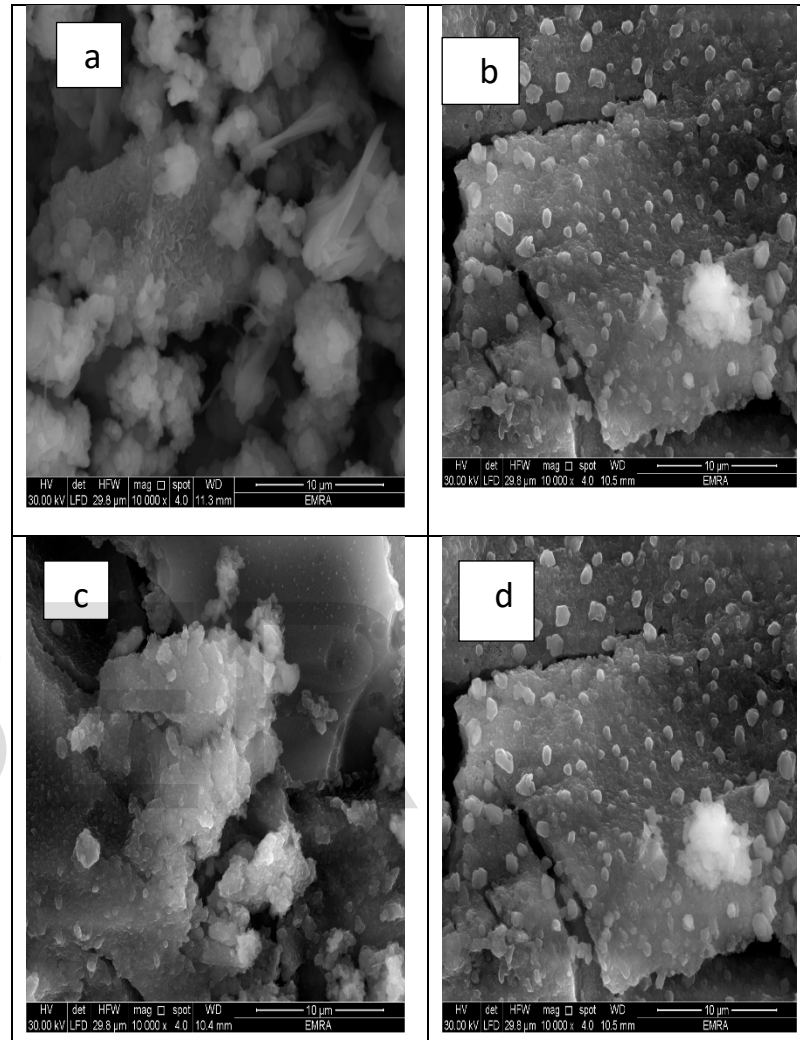
Figure.14. The SEM-micrographs of B1.2 and H1.2 mixes after firing at 200°C and 600°C.


4. Conclusion

The major findings of this work are summarized as follows:

1. The SS:SH ratio plays an important role in the preparation of geopolymer paste, the optimum ratio for SS:SH is 1 while the ratio 0.5 give the least compressive strength values.

2. Partial replacement of slag by 10% Homra increase the compressive strength, enhanced microstructural properties and formed compact geopolymeric structures, where it is increased the rate of Geopolymerisation reaction.

3. Both initial and final setting times increase with decreasing the SS:SH ratio for all tested pastes. Replacing GGBFS with different amount of Homra (10, 20 and 30% by mass of slag) causes a notable increase in both initial and final setting times for GPC specimens made by SS/SH ratio of 2.

4. Water absorption of the formed geopolymers decreased with increasing SS:SH ratio from 0.5 to 1 then showed a slight increase with a further increase to 2.

5. Partial replacement of GGBFS by 10% homra give high strength value than 100% GGBFS as a result of immersion in sulfate solution to evaluate the sulfate attack resistance.

References

[1] D. Roy, Alkali-activated cements opportunities and syntheses, characterization and binding strength of geopolymers: a review challenges, *Cem. Concr. Res. 29*, 1999, 249–254.

[2] S.E. Wallah and B.V. Rangan, *Low-calcium Fly Ash-based Geopolymer Concrete: Longterm Properties*. Research Report GC 2, Faculty of Engineering, Curtin University of Technology, Perth, Australia, 2006.

[3] R. McCaffrey. Climate Change and the Cement Industry, *Environmental overview. GCL Magazine, environmental special issue*. London, UK: Cement Trends; 2002.

[4] J.S.J. van Deventer, J.L. Provis and P. Duxon, Technical and commercial progress in the adoption of geopolymer cement, *Min. Eng. 29,* 2012, 89–104.

[5] J. Davidovits, Properties of geopolymer cements, *Proc. of 1st International Conference on Alkaline Cements and Concretes*, KIEV Ukraine, 1994, pp. 131–149.

[6] E. Mendelovici, Comparative study of the effects of thermal and mechanical treatments on the structures of clay minerals, *J. Therm. Anal. 49 (3)*, 1997, 1385–1397.
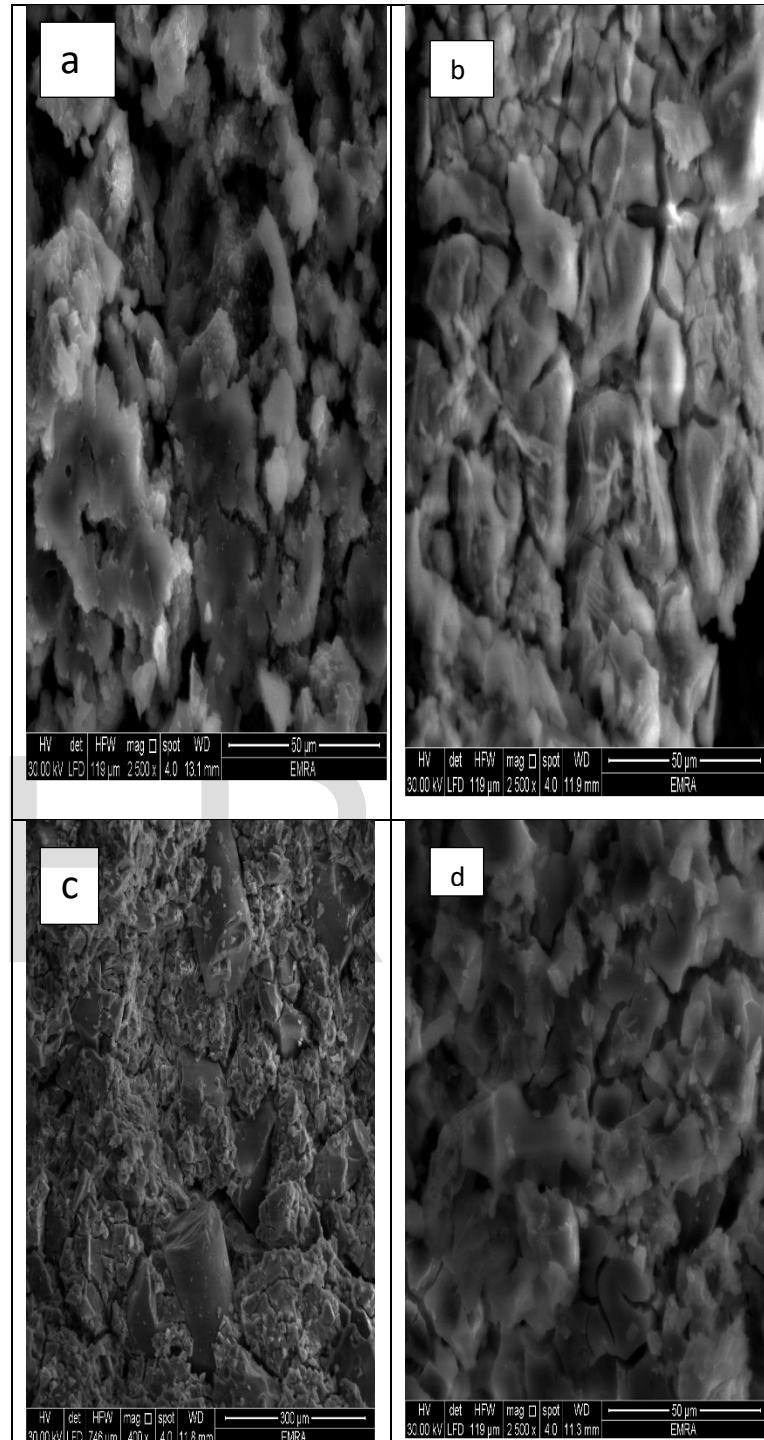
[7] A. Palomo, M.W. Grutzeck and M.T. Blanco, Alkali-activated fly ashes, a cement for the future, *Cem. Concr. Res. 29*, 1999, 1323–1329.

[8] J.Z. Zhang, J.L. Provis, D. Feng and J.S.J. van Deventer, Geopolymers for immobilization of Cr^{6+}, Cd^{2+}, and Pb^{2+}, *J. Hazard. Mater. 157*, 2008, 587–598.

[9] J. Davidovits, Geopolymer chemistry and applications. *3rd ed. France: Geopolymer Institute*; 2011.

[10] J.L. Provis, G.C. Lukey and J.S.J. van Deventer, Do geopolymers actually contain nano crystalline zeolites? A re-examination of existing results, *Chem. Mater. 17*, 2005, 3075–3085.

[11] H. Wang, H. Li and F. Yan, Synthesis and mechanical properties of metakaolinite-based geopolymer, *Colloids Surf. A 268*, 2005, 1–6.

[12] H. Xu and J.S.J. van Deventer, The geopolymerisation of alumino-silicate minerals, *Int. J. Miner. Proc. 59*, 2000, 247–266.

[13] A. Fernandez-Jimenez, A. Palomo and M. Criado, Microstructure development of alkali activated fly ash cement: a descriptive model, *Cem. Concr. Res. 35*, 2005, 1204–1209.

[14] R.A. Robayo, R. Mejia de Gutierrez and M. Gordillo, Natural pozzolan- and granulated blast furnace slag-based binary geopolymers, *Mater. Constr. 66*, 2016, (321).

[15] T. Bakharev, Thermal behaviour of geopolymers prepared using class F fly ash and elevated temperature curing. *Cem. Concr. Res. 36*, 2006, 1134–47.

[16] T. Bakharev, Resistance of geopolymer materials to acid attack. *Cem. Concr. Res. 35*, 2005, 658–70.

[17] T. Bakharev, Durability of geopolymer materials in sodium and magnesium sulfate solutions. *Cem. Concr. Res. 35*, 2005, 1233–46.

[18] T. Bakharev, J. G. Sanjayan and Y. B. Cheng, Resistance of alkali-activated slag concrete to alkali–aggregate reaction. *Cem. Concr. Res. 31*, 2001, 331–40.

[19] T. Bakharev, J. G. Sanjayan and Y. B. Cheng, Resistance of alkali-activated slag concrete to carbonation. *Cem. Concr. Res. 31*, 2001, 1277–83.

[20] J. Davidovits, Geopolymer Chemistry and Applications, Institut Geopolymere, Saint-Quentin, France, 2008.

[21] M. Izquierdo, X. Querol, J. Davidovits, D. Antenucci, H. Nugteren and C. Fernández- Pereira, Coal fly ash-slag-based geopolymers: microstructure and metal leaching, *J. Hazard. Mater. 166 (1)*, 2009, 561–566.

[22] J.G.S. van Jaarsveld and J.S.J. van Deventer, Effect of the alkali metal activator on the properties of fly ash-based geopolymers, *Ind. Eng. Chem. Res. 38 (10)*, 1999, 3932–3941.

[23] V. Živica, Effects of type and dosage of alkaline activator and temperature on the properties of alkali-activated slag mixtures, *Constr. Build. Mater. 21 (7)*, 2007, 1463–1469.

[24] S.A. Bernal, J.L. Provis, V. Rose and R. Mejía de Gutierrez, Evolution of binder structure in sodium silicate-activated slag-metakaolin blends, *Cem. Concr. Compos. 33 (1)*, 2011, 46–54.

[25] W.K.W. Lee and J.S.J. van Deventer, Effects of anions on the formation of aluminosilicate gel in geopolymers, *Ind. Eng. Chem. Res. 41 (18)*, 2002, 4550–4558.

[26] J.J. Chang, A study on the setting characteristics of sodium silicate-activated slag pastes, *Cem. Conr. Res. 33*, 2003, 1005–1011.

[27] C.K. Yip, G.C. Lukey and J.S.J. van Deventer, The coexistence of geopolymeric gel and calcium silicate hydrate at the early stage of alkaline activation, *Cem. Concr. Res. 35 (9)*, 2005, 1688–1697.

[28] S. Alonso and A. Palomo, Alkaline activation of metakaolin and calcium hydroxide mixtures: influence of temperature, activator concentration and solids ratio, *Mater. Lett. 47 (1–2)*, 2001, 55–62.

[29] S. Alonso and A. Palomo, Calorimetric study of alkaline activation of calcium hydroxide– metakaolin solid mixtures, *Cem. Concr. Res. 31 (1)*, 2001, 25–30.

[30] P.J. Williams, J.J. Biernacki, L.R. Walker, H.M. Meyer, C.J. Rawn and J. Bai, Microanalysis of alkali-activated fly ash-CH pastes, *Cem. Concr. Res. 32 (6)*, 2002, 963–972.

[31] C.K. Yip, G.C. Lukey, J.L. Provis and J.S.J. van Deventer, Effect of calcium silicate sources on geopolymerisation, *Cem. Concr. Res. 38 (4)*, 2008, 554–564.

[32] S. Antiohos and S. Tsimas, Activation of fly ash cementitious systems in the presence of quicklime. Part I. Compressive strength and pozzolanic reaction rate, *Cem. Concr. Res. 34 (5)*, 2004, 769–779.

[33] K. Dombrowski, A. Buchwald and M. Weil, The influence of calcium content on the structure and thermal performance of fly ash based geopolymers, *J. Mater. Sci. 42 (9)*, 2007, 3033–3043.

[34] W.K.W. Lee and J.S.J. van Deventer, The effect of ionic contaminants on the early-age properties of alkali-activated fly ash based cements, *Cem. Concr. Res. 32 (4)*, 2002, 577–584.

[35] S. Kumar, R. Kumar and S.P. Mehrotra, Influence of granulated blast furnace slag on the reaction, structure and properties of fly ash based geopolymer, *J. Mater. Sci. 5 (3)*, 2010, 607–615.

[36] C.K. Yip and J.S.J. van Deventer, Microanalysis of calcium silicate hydrate gel formed within a geopolymeric binder, *J. Mater. Sci. 38 (18)*, 2003, 3851–3860.

[37] T.W. Cheng and J.P. Chiu, Fire-resistant geopolymer produced by granulated blast furnace slag, *Miner. Eng. 16 (3)*, 2003, 205–210.

[38] P. De Silva and K. Sagoe-Crenstill, The effect of Al_2O_3 and SiO_2 on setting and hardening of Na_2O–Al_2O_3–SiO_2–H_2O geopolymer systems, *J. Aust. Ceram. Soc. 44 (1)*, 2008, 39–46.

[39] J.J. Chang, A study on the setting characteristics of sodium silicate-activated slag pastes, *Cem. Concr. Res. 33 (7)*, 2003, 1005–1011.

[40] K. Komnitsas, D. Zaharaki and V. Perdikatsis, Effect of synthesis parameters on the compressive strength of low-calcium ferronickel slag inorganic polymers, *J. Hazard. Mater. 161 (2–3)*, 2009, 760–768.

[41] C. Shi, P.V. Krivenko and D. Roy, *Alkali-Activated Cements and Concretes*, Taylor and Francis, Abingdon, UK, 2006.

[42] V.D. Glukhovsky and V.A. Pakhomov, *Slag-Alkali Cements and Concretes*, Budivelnik, Kiev, 1978.

[43] V.D. Glukhovsky (Ed.), *Slag-alkali Concretes Based on Fine-grained Aggregates*, Vishcha Shkola, Kiev, 1981, (in Russian).

[44] P.V. Kruvenko, Alkaline cements, in: *Proc. 1st Int. Conference on Alkali Cement and Concrete*. Kiev, 1994, pp. 11–129.

[45] W. Shao-Dong and S. Karen, Hydration products of alkali activated slag cement, *Cem. Concr. Res. 25*, 1995, 561–571.

[46] H.M. Khater, Effect of cement Kiln dust on geopolymer composition and its resistance to sulfate attack, *Green Mater. J. 1 (1)*, 2013, 36–46.

[47] ASTM C191, Standard Test Methods for Time of Setting of Hydraulic Cement by Vicat Needle, 2013.

[48] E. Rodriguez, S. Bernal, R. Mejia de Gutierrez and F. Puertas, Hormigon alternative basad oenescorias activadasal calinamente, *Mater. Constr. 58 (291)*, 2008, 53–57.

[49] H.K. Tchakoute, A. Elimbi, E. Yanne and C.N. Djangang, Utilization of volcanic ashes for the production of geopolymers cured at ambient temperature, *Cem. Concr. Compos. 38*, 2013, 75–81.

[50] Z. Zhang, H. Wang, Y. Zhu, A. Reid, J. Provis and F. Bullen, Using fly ash to partially substitute metakaolin in geopolymer synthesis, *Appl. Clay Sci. 88–89*, 2014, 194–201.

[51] P. Chindaprasirt, T. Chareerat and V. Sirivivatnanon, Workability and strength of coarse high calcium fly ash geopolymer, *Cem. Concr. Compos. 29*, 2007, 224–229.

[52] S.M.A. El-Gamal and F.A. Selim, Utilization of some industrial wastes for eco-friendly cement production, *Sustainable Materials and Technologies 12*, 2017, 9–17.

[53] L. Reig, M.M. Tashima, M.V. Borrachero, J.Monzo, C.R. Cheeseman and J. Paya, Properties and microstructure of alkali-activated red clay brick waste, *Constr. Build. Mater. 43*, 2013, 98–106.

[54] H. Kamarudin, A.M. Mustafa Al Bakri, M. Binhussain, C.M. Ruzaidi, M. Luqman, C.Y. Heah and Y.M. Liew, Preliminary study on effect of NaOH concentration on early age compressive strength of Kaoline based green cement, *International conference on chemistry and chemical process IPCBEE10*, 2011, pp. 18–24.

[55] P. Duxon, J.L. Provis, G.C. Lukey, S.W. Mallicoat, W.M. Kriven and J.S.J. van Deventer, Colloids Surf. A Physicochem. *Eng. Asp. 269*, 2005, 47–58.

[56] A.M. Mustafa Al Bakri, H. Kamarudin, M. Binhussain, A.R. Rafiza and Y. Zarina, Effect of Na_2SiO_3/NaOH ratios and NaOH molarities on compressive strength of fly-ash based geopolymer, *Mater. J. 109*, 2012, 503–508.

[57] Mechanical and microstructural characterization of geopolymer synthesized from low calcium fly ash, *Chem. Ind. Chem. Eng. Q. 21 (1)*, 2015, 13–22.

[58] H. E. Elyamany, A. M. Abd Elmoaty and A. M. Elshaboury, Magnesium sulfate resistance of geopolymer mortar, *Construction and Building Materials 184*, 2018, 111–127.

[59] F.S. Hashem, Sulphate attack on hardened cement pastes with different porosities in the presence of water- repelling admixtures, *Advanced in Cement Research, 21(2)*, 2009, 75-82.

[60] J. Ye, W. Zhang and D. Shi, Effect of elevated temperature on the properties of geopolymer synthesized from calcined ore-dressing tailing of bauxite and ground-granulated blast furnace slag, *Construction and Building Materials, 69*, 2014, 41–48.

[61] T. Bakharev, Thermal behaviour of geopolymers prepared using class F fly ash and elevated temperature curing. *Cem. Concr. Res., 36(6)*, 2006, 1134–47.

[62] Z. Pan, J. Sanjayan and B.V. Rangan, An investigation of the mechanisms for strength

gain or loss of geopolymer mortar after exposure to elevated temperature, *J Mater Sci 44(7)*, 2009, 1873–1880.

[63] K. DLY and J.G. Sanjayan, Damage behavior of geopolymer composites exposed to elevated temperatures, *Cem. Concr. Compos., 30(10)*, 2008, 986-91.

[64] P. Nath, P.K. Sarker, Effect of GGBFS on setting, workability and early strength properties of fly ash geopolymer concrete cured in ambient condition, *Constr. Build. Mater. 66*, 2014, 163–171.

[65] ASTM C140, Standard Test Methods for Sampling and Testing Concrete Masonry Units and Related Units, 2012.

[66] M. Ben Haha, G. Le Saout, F.Winnefeld and B. Lothenbach, Influence of activator type on hydration kinetics, hydrate assemblage and microstructural development of alkali activated blast-furnace slags, *Cem. Concr. Res. 41 (3)*, 2011, 301–310.

[67] T. Tho-In et al., Compressive strength and microstructure analysis of geopolymer paste using waste glass powder and fly ash, *J. Cleaner Prod. 172*, 2018, 2892–2898.

[68] J.C. Swanepoel and C.A. Strydom, Utilisation of fly ash in a geopolymeric material, *Appl. Geochem. 17 (8)*, 2002, 1143–1148.

[69] A. Fernández-Jiménez and A. Palomo, Composition and microstructure of alkali activated fly ash binder: effect of the activator, *Cem. Concr. Res. 35 (10)*, 2005, 1984–1992.

[70] S. Andini et al., Coal fly ash as raw material for the manufacture of geopolymer-based products, *Waste Manage. (Oxford) 28 (2)*, 2008, 416–423.

[71] D. Panias, I.P. Giannopoulou and T. Perraki, Effect of synthesis parameters on the mechanical properties of fly ash-based geopolymers, *Colloids Surf. A: Physicochem. Eng.Asp. 301 (1)*, 2007, 246–254.

[72] A. Sharmin et al., Influence of source materials and the role of oxide composition on the performance of ternary blended sustainable geopolymer mortar, *Constr. Build. Mater. 144*, 2017, 608–623.

[73] J. Ye, W. Zhang and D. Shi, Properties of an aged geopolymer synthesized from calcined ore-dressing tailing of bauxite and slag, *Cem. Concr. Res. 100 (Suppl. C)*, 2017, 23–31.

[74] M. Tuyan, O. Andic-Çakir and K. Ramyar, Effect of alkali activator concentration and curing condition on strength and microstructure of waste clay brick powder-based geopolymer, *Compos. B Eng. 135*, 2018, 242–252.